EPJ manuscript No.
(will be inserted by the editor)

Hadron Formation in Deep-Inelastic Positron Scattering in a Nuclear Environment

The HERMES Collaboration

A. Airapetian[30], N. Akopov[30], Z. Akopov[30], I. Akushevich[7], M. Amarian[23,25,30], J. Arrington[2], E.C. Aschenauer[7,13,23], H. Avakian[11], R. Avakian[30], A. Avetissian[30], E. Avetissian[30], P. Bailey[15], B. Bains[15], C. Baumgarten[21], M. Beckmann[12], S. Belostotski[24], S. Bernreuther[9], N. Bianchi[11], H. Böttcher[7], A. Borissov[6,14,19], M. Bouwhuis[15], J. Brack[5], S. Brauksiepe[12], B. Braun[9,21], W. Brückner[14], A. Brüll[14,18], P. Budz[9], H.J. Bulten[17,23,29], G.P. Capitani[11], P. Carter[4], P. Chumney[22], E. Cisbani[25], G.R. Court[16], P.F. Dalpiaz[10], R. De Leo[3], L. De Nardo[1], E. De Sanctis[11], D. De Schepper[2,18], E. Devitsin[20], P.K.A. de Witt Huberts[23], P. Di Nezza[11], V. Djordjadze[7], M. Düren[9], A. Dvoredsky[4], G. Elbakian[30], J. Ely[5], A. Fantoni[11], A. Fechtchenko[8], L. Felawka[27], M. Ferro-Luzzi[23,29], K. Fiedler[9], B.W. Filippone[4], H. Fischer[12], B. Fox[5], J. Franz[12], S. Frullani[25], Y. Gärber[7], F. Garibaldi[25], E. Garutti[10,23], G. Gavrilov[24], V. Gharibyan[30], A. Golendukhin[6,21,30], G. Graw[21], O. Grebeniouk[24], P.W. Green[1,27], L.G. Greeniaus[1,27], A. Gute[9], W. Haeberli[17], M. Hartig[27], D. Hasch[7,11], D. Heesbeen[23], F.H. Heinsius[12], M. Henoch[9], R. Hertenberger[21], W.H.A. Hesselink[23,29], G. Hofman[5], Y. Holler[6], R.J. Holt[15], B. Hommez[13], G. Iarygin[8], M. Iodice[25], A. Izotov[24], H.E. Jackson[2], A. Jgoun[24], P. Jung[6], R. Kaiser[7,26,27], J. Kanesaka[28], E. Kinney[5], A. Kisselev[24], P. Kitching[1], H. Kobayashi[28], N. Koch[9], K. Königsmann[12], H. Kolster[21,23], V. Korotkov[7], E. Kotik[1], V. Kozlov[20], V.G. Krivokhijine[8], G. Kyle[22], L. Lagamba[3], A. Laziev[23,29], P. Lenisa[10], T. Lindemann[6], W. Lorenzon[19], N.C.R. Makins[2,15], J.W. Martin[18], H. Marukyan[30], F. Masoli[10], M. McAndrew[16], K. McIlhany[4,18], R.D. McKeown[4], F. Meissner[7], F. Menden[12], A. Metz[21], N. Meyners[6], O. Mikloukho[24], C.A. Miller[1,27], R. Milner[18], V. Muccifora[11], R. Mussa[10], A. Nagaitsev[8], E. Nappi[3], Y. Naryshkin[24], A. Nass[9], K. Negodaeva[7], W.-D. Nowak[7], K. Oganessyan[11], T.G. O'Neill[2], R. Openshaw[27], J. Ouyang[27], B.R. Owen[15], S.F. Pate[18,22], S. Potashov[20], D.H. Potterveld[2], G. Rakness[5], V. Rappoport[24], R. Redwine[18], D. Reggiani[10], A.R. Reolon[11], R. Ristinen[5], K. Rith[9], D. Robinson[15], A. Rostomyan[30], M. Ruh[12], D. Ryckbosch[13], Y. Sakemi[28], T. Sato[28], I. Savin[8], C. Scarlett[19], A. Schäfer[31] C. Schill[12], F. Schmidt[9], G. Schnell[22], K.P. Schüler[6], A. Schwind[7], J. Seibert[12], B. Seitz[1,27], T.-A. Shibata[28], T. Shin, V. Shutov[8], M.C. Simani[10,23,29], A. Simon[12], K. Sinram[6], E. Steffens[9], J.J.M. Steijger[23], J. Stewart[16,27], U. Stösslein[5,7], K. Suetsugu[28], M. Sutter[18], S. Taroian[30], A. Terkulov[20], S. Tessarin[10], E. Thomas[11], B. Tipton[18,4], M. Tytgat[13], G.M. Urciuoli[25], J.F.J. van den Brand[23,29], G. van der Steenhoven[23], R. van de Vyver[13], J.J. van Hunen[23], M.C. Vetterli[26,27], V. Vikhrov[24], M.G. Vincter[1,27], J. Visser[23], E. Volk[14], C. Weiskopf[9], J. Wendland[26,27], J. Wilbert[9], T. Wise[17], S. Yen[27], S. Yoneyama[28], H. Zohrabian[30]

[1] Department of Physics, University of Alberta, Edmonton, Alberta T6G 2J1, Canada[c]
[2] Physics Division, Argonne National Laboratory, Argonne, Illinois 60439-4843, USA[d]
[3] Istituto Nazionale di Fisica Nucleare, Sezione di Bari, 70124 Bari, Italy
[4] W.K. Kellogg Radiation Laboratory, California Institute of Technology, Pasadena, California 91125, USA[e]
[5] Nuclear Physics Laboratory, University of Colorado, Boulder, Colorado 80309-0446, USA[f]
[6] DESY, Deutsches Elektronen Synchrotron, 22603 Hamburg, Germany
[7] DESY Zeuthen, 15738 Zeuthen, Germany
[8] Joint Institute for Nuclear Research, 141980 Dubna, Russia
[9] Physikalisches Institut, Universität Erlangen-Nürnberg, 91058 Erlangen, Germany[g,h]
[10] Istituto Nazionale di Fisica Nucleare, Sezione di Ferrara and Dipartimento di Fisica, Università di Ferrara, 44100 Ferrara, Italy
[11] Istituto Nazionale di Fisica Nucleare, Laboratori Nazionali di Frascati, 00044 Frascati, Italy
[12] Fakultät für Physik, Universität Freiburg, 79104 Freiburg, Germany[g]
[13] Department of Subatomic and Radiation Physics, University of Gent, 9000 Gent, Belgium[i]
[14] Max-Planck-Institut für Kernphysik, 69029 Heidelberg, Germany
[15] Department of Physics, University of Illinois, Urbana, Illinois 61801, USA[j]
[16] Physics Department, University of Liverpool, Liverpool L69 7ZE, United Kingdom[k]
[17] Department of Physics, University of Wisconsin-Madison, Madison, Wisconsin 53706, USA[l]
[18] Laboratory for Nuclear Science, Massachusetts Institute of Technology, Cambridge, Massachusetts 02139, USA[m]
[19] Randall Laboratory of Physics, University of Michigan, Ann Arbor, Michigan 48109-1120, USA[n]
[20] Lebedev Physical Institute, 117924 Moscow, Russia
[21] Sektion Physik, Universität München, 85748 Garching, Germany[g]

[22] Department of Physics, New Mexico State University, Las Cruces, New Mexico 88003, USA[o]
[23] Nationaal Instituut voor Kernfysica en Hoge-Energiefysica (NIKHEF), 1009 DB Amsterdam, The Netherlands[p]
[24] Petersburg Nuclear Physics Institute, St. Petersburg, Gatchina, 188350 Russia
[25] Istituto Nazionale di Fisica Nucleare, Sezione Sanità and Physics Laboratory, Istituto Superiore di Sanità, 00161 Roma, Italy
[26] Department of Physics, Simon Fraser University, Burnaby, British Columbia V5A 1S6, Canada[c]
[27] TRIUMF, Vancouver, British Columbia V6T 2A3, Canada[c]
[28] Department of Physics, Tokyo Institute of Technology, Tokyo 152, Japan[q]
[29] Department of Physics and Astronomy, Vrije Universiteit, 1081 HV Amsterdam, The Netherlands[p]
[30] Yerevan Physics Institute, 375036, Yerevan, Armenia
[31] Institut für Theoretische Physik, Universität Regensburg, 93040 Regensburg, Germany

[a] supported by INTAS contract No. 93-1827
[b] partially supported by the Thomas Jefferson National Accelerator Facility, under DOE contract DE-AC05-84ER40150.
[c] supported by the Natural Sciences and Engineering Research Council of Canada (NSERC)
[d] supported by the US Department of Energy, Nuclear Physics Div., grant No. W-31-109-ENG-38
[e] supported by the US National Science Foundation, grant No. PHY-9420470
[f] supported by the US Department of Energy, Nuclear Physics Div., grant No. DE-FG03-95ER40913
[g] supported by the Deutsche Bundesministerium für Bildung, Wissenschaft, Forschung und Technologie
[h] supported by the Deutsche Forschungsgemeinschaft
[i] supported by the FWO-Flanders, Belgium
[j] supported by the US National Science Foundation, grant No. PHY-9420787
[k] supported by the U.K. Particle Physics and Astronomy Research Council
[l] supported by the US Department of Energy, Nuclear Physics Div., grant No. DE-FG02-88ER40438, and the US National Science Foundation, grant No. PHY-9722556
[m] supported by the US Department of Energy, Nuclear Physics Division
[n] supported by the US National Science Foundation, grant No. PHY-9724838
[o] supported by the US Department of Energy, Nuclear Physics Div., grant No. DE-FG03-94ER40847
[p] supported by the Dutch Foundation for Fundamenteel Onderzoek der Materie (FOM)
[q] supported by Monbusho, JSPS and Toray Science Foundation of Japan

Received: May 3, 2001

Abstract. The influence of the nuclear medium on the production of charged hadrons in semi-inclusive deep-inelastic scattering has been studied by the HERMES experiment at DESY using a 27.5 GeV positron beam. The differential multiplicity of charged hadrons and identified charged pions from nitrogen relative to that from deuterium has been measured as a function of the virtual photon energy ν and the fraction z of this energy transferred to the hadron. There are observed substantial reductions of the multiplicity ratio R_M^h at low ν and at high z, both of which are well described by a gluon-bremsstrahlung model of hadronization. A significant difference of the ν-dependence of R_M^h is found between positive and negative hadrons. This is interpreted in terms of a difference between the formation times of protons and pions, using a phenomenological model to describe the ν- and z-dependence of R_M^h.

1 Introduction

In deep-inelastic scattering (DIS) an incident lepton interacts with a target via the exchange of a gauge boson between the lepton and a parton (a quark or an antiquark). The struck parton is subjected to a sequence of hard parton- and soft hadron-production processes, resulting in the formation of hadrons. By carrying out DIS experiments on nuclear targets, it is possible to study the hadronization process during the time period immediately after the quark has been struck by the virtual photon [1]. In the simplest scenario the nucleus, which has the size of a few fm, acts as an ensemble of targets with which the struck quark or the produced hadron may interact. If an interaction occurs, the number of leading hadrons produced per DIS event and per nucleon is reduced compared to that for a free nucleon. The reduction of hadron multiplicity depends on the distance traversed by the struck quark before the hadron is formed, the (unknown) quark-nucleon cross section and the (known) hadron-nucleon cross section. Hence, measurements of the multiplicity of hadrons produced on nuclei can provide information on the space-time structure of the hadronization process.

In this paper we present the results of deep-inelastic positron scattering measurements on ^{14}N and ^{2}H targets carried out by the HERMES Collaboration at DESY. The reduction of the hadron multiplicity on ^{14}N relative to that on ^{2}H has been determined from the data. Deuterium was used as a reference target instead of hydrogen to account for the difference in scattering from neutrons or protons.

In the past, semi-inclusive leptoproduction of hadrons from nuclei was studied at SLAC with electrons [2] and at CERN and FNAL with high-energy muons by EMC [3] and E665 [4]. In these experiments the effect of the nucleus on the early stages of hadronization appeared in the dependence of the multiplicity ratios on the energy ν of the virtual photon (as defined in the target rest frame).

The effect is most prominent if ν ranges from a few GeV to a few tens of GeV. The ν-range covered by the present experiment (7 – 23 GeV was used in the present analysis) is low enough to be optimal for studying the influence of the nuclear medium on the hadronization process, while it is still high enough to be in the scaling regime, i.e. for the DIS-framework to apply.

2 Model calculations

The theoretical description of hadronization is difficult, as it is impossible to treat the problem in a perturbative QCD-framework. Although the nuclear environment can be used to study certain aspects of the hadron formation process, the same difficulties apply to the description of nuclear effects on hadronization. Therefore, one has to resort to model calculations. The HERMES data on hadron production from nuclei are compared to the gluon-bremsstrahlung-model calculations of Ref. [5], and the phenomenological intranuclear reinteraction model of Refs. [6, 7].

In the gluon-bremsstrahlung model, the struck quark is assumed to lose energy via the emission of gluons until, in the case of meson formation, a $q\bar{q}$ configuration is formed consisting of the struck quark and an antiquark originating from the last emitted gluon [5, 8–10]. If this last step occurs inside the nucleus, the nuclear environment affects the hadron multiplicity because the meson interacts with the nuclear medium with a sizable cross section. Moreover, the interaction of the initial quark with the nuclear medium causes the emission of additional soft gluons. On the other hand, the initial — possibly small — $q\bar{q}$ configuration represents a color dipole which may have a reduced probability of interaction with its environment (Color Transparency [11, 12]). An estimate of the combined effect of the soft gluon radiation and Color Transparency on the multiplicity ratio in the framework of the gluon-bremsstrahlung model [5] yields 2–3% for the kinematics of the present experiment.

An important parameter characterizing the hadronization process is the formation time (in the target rest frame) t_f^h, which is defined as the mean time elapsed between the moment the quark is struck and the creation of the leading hadron h. In the gluon-bremsstrahlung model [5], the probability distribution of t_f^h may be evaluated for given values of z and ν, where z represents the fraction of the energy ν transferred to the hadron. The mean value of t_f^h exhibits an approximate $(1-z)\nu$-dependence. In the phenomenological models [6, 7], on the other hand, the formation time is assumed to be equal to the product of a time constant τ_h intrinsic to the kind of hadron produced, and a time-dilation factor ν/m where m represents a mass. In the past, several functional forms for t_f^h have been considered [6, 7, 11, 13–15] — for instance $t_f^h = \tau_h z\nu/m_h$ or $t_f^h = \tau_h \nu/m_q$, where m_h (m_q) represents the mass of the hadron (constituent quark). Alternatively, one may take for m the kinematic expression derived by Berger [16] for the mass of the offshell struck (current) quark. Under the assumption that the mass of the initial quark and that of the produced hadron can be neglected, one finds $t_f^h = \tau_h \sqrt{z(1-z)/p_T^2}\nu$, where p_T represents the component of the hadron momentum transverse to the direction of the virtual-photon momentum.

3 Experiment

The experimental results are presented in terms of the multiplicity ratio R_M^h, which represents the ratio of the number of hadrons of type h produced per DIS event for a nuclear target of mass A to that from a deuterium target (D):

$$R_M^h(z,\nu) = \frac{N_h^A(z,\nu)}{N_e^A(\nu)} \Big/ \frac{N_h^D(z,\nu)}{N_e^D(\nu)} \qquad (1)$$

with $N_h(z,\nu)$ the number of semi-inclusive hadrons in a given (z,ν)-bin, and $N_e(\nu)$ the number of inclusive DIS positrons in the same ν-bin. For the purpose of the present analysis, the multiplicity ratio was determined as a function of ν and z, while integrating over all other kinematic variables. The data for R_M^h are only weakly dependent on either Q^2 or p_T^2 [25].

The HERMES experiment at DESY makes use of the 27.5 GeV positron storage ring of HERA. The ^{14}N and ^{2}H target gases are injected into a tubular open-ended storage cell through which the beam passes. The cell provides a 40 cm long target with areal densities of up to 6×10^{15} nucleons/cm^2 for ^{14}N. The dead time of the data acquisition system was observed to be less than 5% even at the highest luminosities of about 10^{33} cm^{-2}s^{-1}.

In the HERMES spectrometer [17] both the scattered positrons and the produced hadrons are detected and identified within an angular acceptance of ± 170 mrad horizontally, and ± (40 – 140) mrad vertically. The trigger for scattered positrons was formed from a coincidence between several scintillator hodoscope planes and a lead-glass calorimeter. The trigger required an energy of more than 3.5 GeV deposited locally in the calorimeter. Positron identification was accomplished using the calorimeter, the second hodoscope, which functioned as a preshower counter, a transition-radiation detector, and a threshold gas Čerenkov counter filled with a mixture of N_2 and C_4F_{10} at atmospheric pressure. This system provided positron identification with an average efficiency of 99 % and a hadron contamination of less than 1 %. Hadrons with an energy $E_h \geq 1.4$ GeV could be distinguished from leptons. Furthermore, in the momentum range between 4 and 13.5 GeV, pions were identified with the help of the Čerenkov counter.

4 Data analysis

Events were selected by imposing constraints on the four-momentum squared $-Q^2$ of the virtual photon, the invariant mass of the photon-nucleon system W, the Bjorken

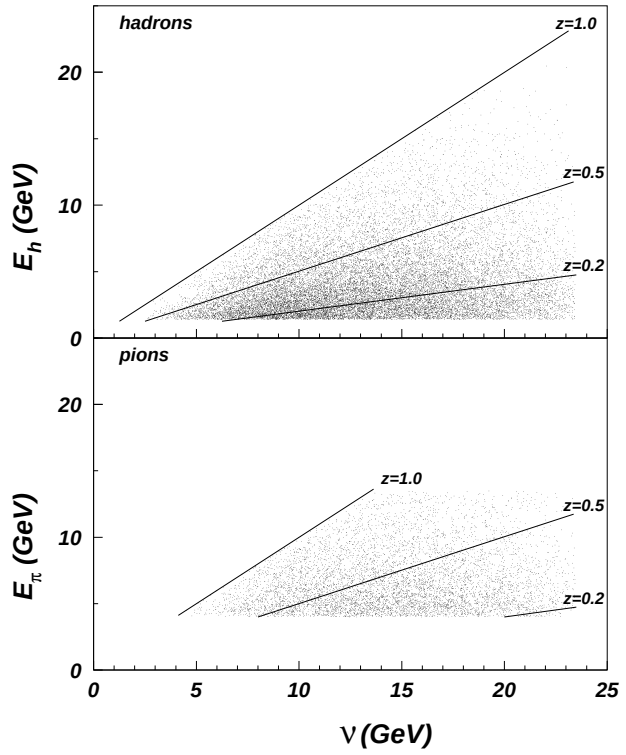

Fig. 1. Scatter plot of the hadron (or pion) energy E_h (E_π) and the energy transfer ν. Lines representing constant values of z are shown as well.

scaling variable $x = \frac{Q^2}{2m_p\nu}$ (with m_p the proton mass), and the energy fraction of the virtual photon $y = \nu/E_{beam}$. For each event it was required that $x > 0.06$, $Q^2 > 1$ GeV^2, $W > 2$ GeV, and $y < 0.85$. The requirements on W and y are applied to exclude nucleon resonances and to limit the magnitude of the radiative corrections, respectively. The constraints on (x, Q^2) are applied to exclude the kinematic region where an anomalous ratio of the longitudinal to transverse cross sections for inclusive deep-inelastic scattering from ^{14}N has been observed [18]. The anomaly can be interpreted as being due to the absorption of the virtual photon by a correlated quark pair [19] or by a nuclear meson [20]. Either interpretation breaches the assumption of incoherent lepton-quark scattering, inherent in deep-inelastic scattering.

The instrumental threshold on E_h is larger for pions than for hadrons. This implies, as is illustrated in Fig. 1, that e.g. the pion z-acceptance is restricted to rather large values as ν decreases. Hence, to ensure that the ν-dependence of the multiplicity ratio does not correspond to a strong variation of the mean z-value, the presented data are confined to $z > 0.2$ and $\nu > 7$ GeV for hadrons and $z > 0.5$ and $\nu > 8$ GeV for pions.

Under the kinematic constraints described above, the number of selected DIS events is 0.88 (1.05) $\times 10^6$ for ^{14}N (^{2}H) if $\nu > 7$ GeV. For $\nu > 8$ GeV these numbers decrease to 0.76 $\times 10^6$ for ^{14}N and 0.91 $\times 10^6$ for ^{2}H. The number of hadrons with $z > 0.2$ equals 227 (288) $\times 10^3$, and the number of pions with $z > 0.5$ is 36 (48) $\times 10^3$ for ^{14}N (^{2}H).

The HERMES data have been corrected for radiative processes using the codes of Refs. [21,22]. As is commonly done [2,3], the contributions from nuclear elastic scattering, quasi-elastic scattering and DIS were treated independently. Coherence-length effects [23] are not included in this approach. The code of Ref. [22] was modified to include the measured semi-inclusive DIS cross sections for ^{14}N. The size of the radiative correction was found to be negligible in most of the kinematic range, with a maximum of 3% at the highest value of ν. The correction is so small because most of the contributions to the radiative corrections cancel in the multiplicity ratio.

The systematic uncertainty of the present data is 3% or less. The uncertainty is small due to the fact that double ratios of semi-inclusive and inclusive yields are measured. The main contributions to the systematic uncertainty arise from radiative corrections ($< 2\%$), overall efficiency ($< 1.5\%$), and diffractive ρ^0-meson production ($<1.5\%$) [25]. It has been verified that the acceptance for semi-inclusive hadron production is the same for both targets, by plotting the multiplicity ratio versus hadron angle and p_T^2. These ratios are constant to within the expected statistical precision except for the data beyond $p_T^2 = 1$ GeV^2, where an enhancement similar to that reported by Ref. [3] is observed. Because of the steep decline of semi-inclusive hadron production with p_T^2, this enhancement does not contribute to the present data. The nuclear attenuation of pions resulting from the decay of ρ-mesons formed in the fragmentation process (which constitute about 20% of the semi-inclusive pion yield) was found to have a ν-dependence similar to that of the direct-fragmentation pions. No correction for this process was therefore applied.

5 Results

The results for the multiplicity ratio for all charged hadrons with $z > 0.2$ are presented as a function of ν in Fig. 2 together with data of previous experiments. In the top panel, existing data on copper [2,3] are shown together with the original phenomenological calculations that were used to interpret the data. In the lower panel of Fig. 2, the present data on ^{14}N are displayed together with data of previous experiments at CERN [3] and SLAC [2] on ^{12}C. The SLAC data point is lower than the present data by five standard deviations. For the SLAC data no systematic uncertainty is available from the original publication. Moreover, no corrections were made for the target-mass dependence of the inclusive DIS cross section, an effect that was not known at the time of the analysis. Such a correction is needed because a semi-inclusive cross-section ratio was measured at SLAC instead of the multiplicity ratio defined in Eq. (1). An estimate of the correction for this effect – based on the HERMES ^{14}N data – results in a 4% increase of R_M^h, which reduces the discrepancy by a factor of two.

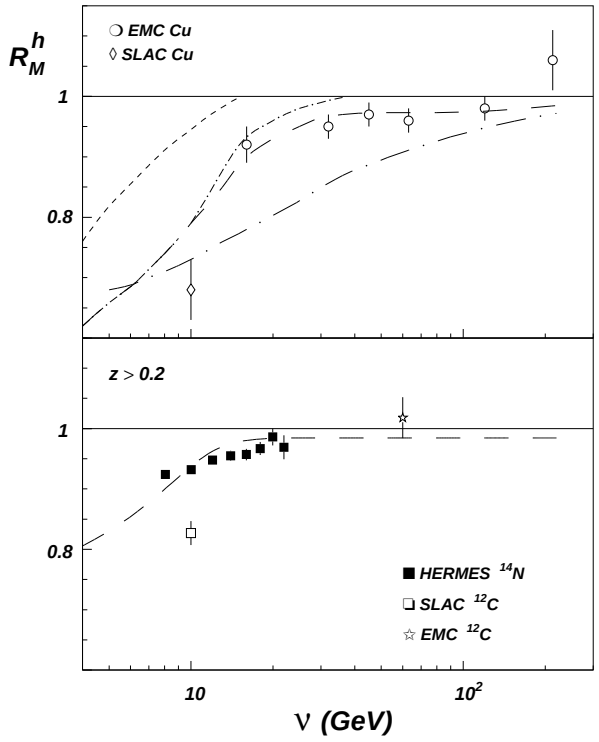

Fig. 2. Charged hadron multiplicity ratio R_M^h as a function of ν for values of z larger than 0.2. In the upper panel the CERN [3] and SLAC [2] data for Cu are compared to various phenomenological calculations taken from the original publications [3, 15]. In the lower panel the HERMES data on ^{14}N are represented by solid squares, while the open star represents the CERN data point on ^{12}C and the open square the SLAC data point on ^{12}C. The error bars represent the statistical uncertainty only. The systematic uncertainty of the HERMES data is $\leq 3\%$. The curves are described in the text.

The present data for R_M^h are observed to increase with increasing ν and approach unity for high ν, which is consistent with the EMC data. This behaviour suggests that for large values of ν, hadron formation takes place mainly outside the ^{14}N nucleus, and that the interaction of the struck quark with the nuclear medium is weak.

Table 1. Parameters used in the phenomenological one and two time-scale model calculations shown in Figs. 2 and 3. In the left two columns the line type used in the figures and the expression used for the formation time are listed, while the three columns on the right give the values of the three cross sections (in mb) used in the calculations.

line type	t_f^h (fm/c)	σ_q	σ_s	σ_h
— · — · —	$c_h \times z\nu$	0	–	20
— — — —	$(1-\ln(z))z\nu/(\kappa c)$	0.75	20	20
- - - - - - -	$(1-\ln(z))z\nu/(\kappa c)$	0	20	20
- - - - - - -	$(1-\ln(z))z\nu/(\kappa c)$	0	0	20
· · · · · · · · ·	$c_h \times (1-z)\nu$	0	- -	25

For the interpretation of the data it is useful to provide some details on the calculations from Ref. [3] shown in the upper panel of Fig. 2. Similar calculations are also used when discussing the z-dependence of the ^{14}N data below. The long-dash dotted curve represents a calculation in the framework of the one time-scale model [6], in which it is assumed that the influence of the nuclear medium on the hadron multiplicity is due to quark-nucleon scattering for $t < t_f^h$ and hadron-nucleon scattering for $t > t_f^h$, with cross sections σ_q and σ_h respectively. In the calculation shown $t_f^h = c_h z\nu$ with $c_h = 1$ fm/(GeVc) [11] has been assumed, and the parameters listed in table 1 have been used. The other curves in fig. 2 are three examples of two time-scale model calculations, in which the formation time is assumed to be given by $t_f^h = (1-\ln(z))z\nu/(\kappa c)$ with c the speed of light and $\kappa \approx 1$ GeV/fm the string tension [7, 13]. In these models an additional parameter σ_s is introduced that represents the interaction between the open string and the medium occurring after a time interval $\tau_c = t_f^h - z\nu/(\kappa c)$. The expressions for t_f^h and τ_c have been derived from the color-string model [24]. The parameters used for the three calculations shown are also listed in table 1. The long-dashed curves give a fairly good description of both the Cu and the present ^{14}N data. However, it should be noted that a two time-scale model calculation with $\sigma_s = \sigma_h$ is equivalent to a one time-scale model calculation except with a different expression for t_f^h. For this reason we will use only the one time-scale model when presenting the final parameterization of the data near the end of this paper.

5.1 z-dependence

In order to further investigate the various possible descriptions of the hadron formation process, the z-dependence of R_M^h was extracted from the present measurements for both hadrons and identified pions. The multiplicity ratio for hadrons (pions) with $\nu > 7$ GeV (8 GeV) is presented as a function of z in Fig. 3.

No significant difference between data for hadrons and pions is observed here. The decrease of R_M^h with z, as observed at $z > 0.8$ for the first time by the present experiment, is at variance with the phenomenological-model calculations, which predict an increase of R_M^h with z. This is demonstrated by the long-dash-dotted (one time-scale) and long-dashed (two time-scale) calculations shown in Fig. 3. The curves have been obtained in the same way as the corresponding curves in Fig. 2 only using the ^{14}N matter density instead of the one for Cu. It is concluded that the (z,ν)-dependence of the formation time is not given by the simple expressions [6, 11] mentioned above. It is significant that the expression for t_f^h implied by the kinematic z-dependence of the invariant mass of the current quark [16] also fails to reproduce the observed dependence of R_M^h on either z or p_T^2 [3, 15].

The solid curve, on the other hand, gives a good account of the data. It represents the result of a calculation for R_M^π within the gluon-bremsstrahlung model [5]. Note

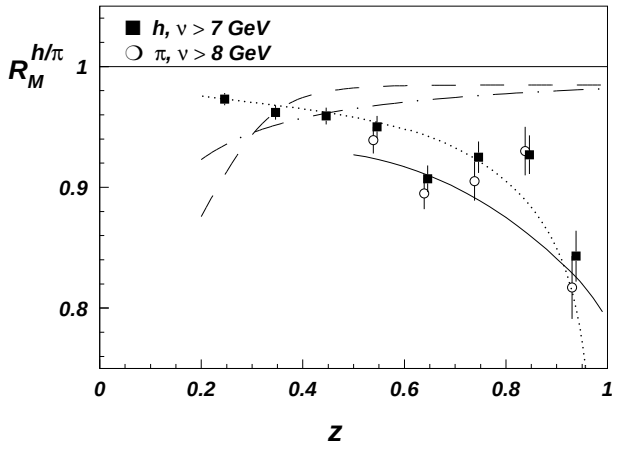

Fig. 3. The multiplicity ratio as a function of z for all charged pions (open circles) and all charged hadrons including pions (closed squares). The full curve represents a gluon-bremsstrahlung model calculation for pions. The dotted, dashed and dot-dashed curves represent phenomenological formation-time calculations.

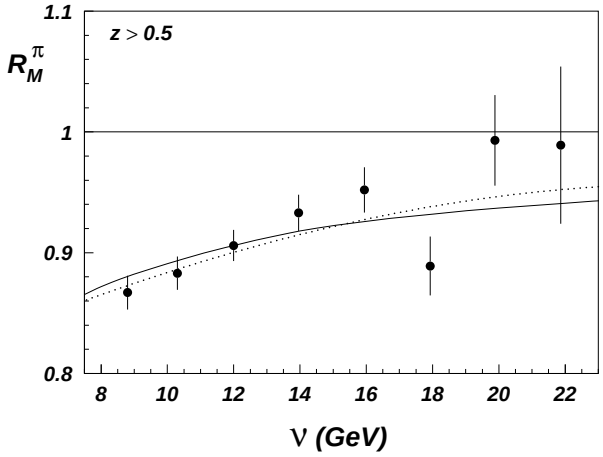

Fig. 4. The multiplicity ratio as a function of ν for charged pions with $z > 0.5$. The solid curve represents a gluon-bremsstrahlung model calculation. The dotted curve is the result of a one time-scale model calculation assuming a $(1-z)\nu$-dependence of the formation time.

that the calculation applies to pions only. The basic mechanism that causes the decrease of R_M^h at large values of z is the following. A hadron with large z originates from a quark that has emitted only few gluons of relatively small energy; otherwise its z-value would have been lower. As the bare quark continuously emits gluons, the emission of only few gluons correlates with small formation times. Hence, the probability that the high-z hadron is subject to rescattering is largest, explaining the decrease of R_M^h at high z. It is noted that a similar reduction of hadroproduction data at large x_F ($\approx z$) requires a more involved theoretical treatment [7, 26].

In order to be able to study phenomenological concepts such as the quark-nucleon cross section σ_q and the formation time t_f^h, the z-dependence of R_M^h has been parameterized in the framework of the one time-scale model. Using the expression $t_f^h = c_h(1-z)\nu$, as suggested by the gluon-bremsstrahlung model [5] and the string string-model calculation of Ref. [27], the dotted curve in Fig. 3 has been obtained. It represents the result of a fit with the factor c_h a free parameter, and σ_q and σ_h set to the values listed in table 1. It is concluded that a phenomenological description of the z-dependence of the R_M^h data can be obtained if an ad-hoc $(1-z)$-dependence of the formation time is assumed.

5.2 ν-dependence

The ν-dependence of the multiplicity ratio for charged pions with $z > 0.5$ is shown in Fig. 4. The calculation with the gluon-bremsstrahlung model [5] is in fair agreement with the data. A similar description of the data is obtained using the one time-scale model with $t_f^\pi = c_\pi(1-z)\nu$, assuming $\sigma_q = 0$ mb and $\sigma_h = 25$ mb (dotted curve in Fig. 4). In a two-parameter fit with c_π and σ_q treated as free parameters, the resulting value for σ_q is consistent with zero with an uncertainty of only ± 0.4 mb (or ± 0.2 mb if the hadrons are considered). It is concluded that in the context of the phenomenological models, the interaction of the struck quark with the nuclear medium is indeed very small, which is in accordance with the results of Refs. [5, 15]. Hereafter, we extract further information about the hadron formation time within the context of the one time-scale model with $\sigma_q \approx 0$.

5.3 Hadron-charge dependence

The results presented thusfar concern the sum of positive and negative hadrons. For both pions and hadrons the charge states can be studied separately. In the upper (lower) panel of Fig. 5, the multiplicity ratios for positive and negative hadrons (pions) are displayed as a function of ν. The same requirements on the variable ν as before have been imposed: $\nu > 7$ GeV for the hadron data and $\nu > 8$ GeV for the pion data. However, for the purpose of this comparison and in order to increase the pion statistics, the requirement $z > 0.2$ has been imposed in both cases.

The data show that the multiplicity ratio R_M^π is the same for positive and negative pions. This observation — together with the fact that the $\pi^\pm$–N interaction cross sections are about equal — is consistent with the likely assumption that the formation times for the two charge states are the same.

In contrast, a significant difference is observed between R_M^h of positive and negative hadrons. Since the multiplicity ratios of positive and negative pions are measured to be equal, this difference must be caused by other hadrons, such as protons, antiprotons and kaons. A Monte Carlo study with the LUND model [28] has been performed in order to estimate the relative yield of various hadrons in

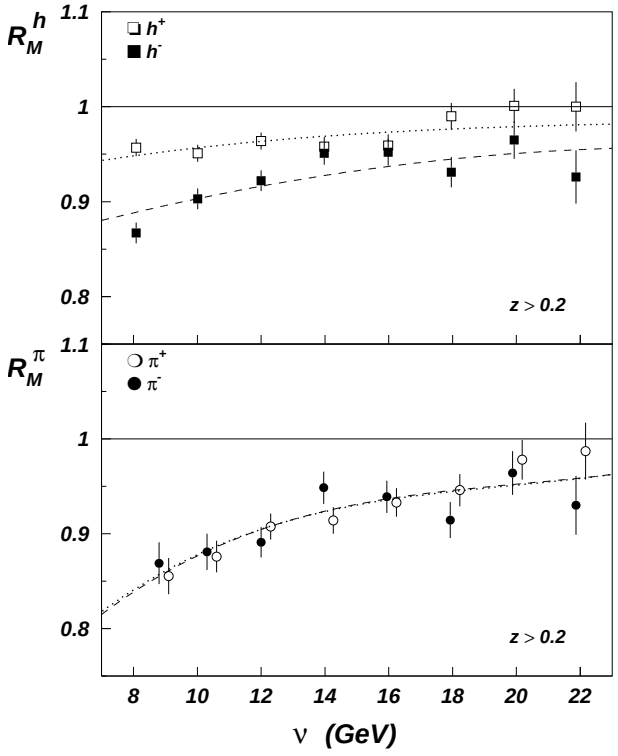

Fig. 5. Multiplicity ratios for hadrons including pions (top panel) and identified pions (bottom panel) as a function of ν. The open (closed) squares represent the positive (negative) hadrons. Identified pions are represented by open (positive) and closed (negative) circles. The curves are parameterizations of the data using the one time-scale model assuming $t_f^h = c_h(1-z)\nu$.

the acceptance of the spectrometer. The study shows that the contribution of antiprotons (protons) to the negative (positive) hadron sample, averaged in the ν-range of 3 – 23 GeV, equals 6% (24%). In the same kinematic range, the negative and positive kaon contributions are 10 and 13%, respectively. Since the effects of the interaction between the struck quark and the nuclear medium are found to be small, only two effects may account for the observed difference between R_M^{h+} and R_M^{h-}: the difference in the cross sections [29] for rescattering of antiprotons ($\approx$ 60 mb), protons ($\approx$ 40 mb), negative kaons ($\approx$ 23 mb) and positive kaons ($\approx$ 17 mb), or possible differences between the formation times of baryons and mesons. Noting that the effective hadron-nucleon cross sections, obtained as the weighted sum of individual hadron cross sections, are practically the same for the positive and negative hadron samples, the observed difference of R_M^{h+} and R_M^{h-} is most likely due to differences in the formation times of pions, kaons and/or (anti)protons. Since the proton fraction in the positive hadron sample is four times larger than the antiproton fraction in the negative hadron sample, it is concluded that protons have a significantly larger formation time than pions. In order to substantiate this conclusion, additional data with good pion, kaon and proton identification are needed.

5.4 Discussion

In the absence of a theoretical model predicting the observed difference between R_M^{h+} and R_M^{h-}, the data of Fig. 5 have been parameterized using the one time-scale model [6]. In these calculations, the formation time is assumed to be given by $t_f^h = c_h(1-z)\nu$ to ensure a proper description of the z-dependence of R_M^h, and an effective hadron-nucleon cross section of 25 mb is used for all hadrons. Initially both σ_q and c_h were used as free parameters. In all four cases (h^+, h^-, π^+, and π^-) the fits gave a good account of the data, while the fitted value of σ_q was found to be consistent with zero within uncertainties ranging from 0.3 mb for π^+ to 1.2 mb for h^-. This implies that the dominant effect of the nucleus on R_M^h is due to hadron-nucleon interactions. Setting σ_q equal to zero, the fits were repeated yielding once more a good description of the data (see Fig. 5) and the following set of fit parameters: $c_{\pi^-} = 1.38\pm0.21$ fm/(GeVc), $c_{\pi^+} = 1.37\pm0.18$ fm/(GeVc), $c_{h^-} = 1.32\pm0.16$ fm/(GeVc), and $c_{h^+} = 3.49\pm0.51$ fm/(GeVc). The quoted uncertainties equal the quadratic sum of the statistical errors of the fit parameters and the variations of these parameters when the hadron-nucleon cross section is varied by ±2 mb. The fitted values of c_h quantitatively confirm our earlier conclusions concerning the equality of the formation times of positive and negative pions, and the large difference between the formation times of positive and negative hadrons.

6 Summary

In summary, high accuracy data on the attenuation of charged hadrons and identified pions in deep-inelastic scattering on ^{14}N relative to ^{2}H have been obtained by the HERMES experiment. The ν-dependence of the multiplicity ratio of hadrons (h^+ and h^-) has a similar behaviour as the CERN muon [3] data. In the previously unexplored high z-region covered by the present experiment, a decrease of R_M^h with z is observed. This observation is in agreement with the prediction of the gluon bremsstrahlung model [5], but is at variance with the prescription often used in phenomenological models that the hadron formation time is proportional to z, and with the z-dependence implied by Ref. [16]. In contrast to what is observed for positive and negative pions, a difference is found in the ν-dependence of R_M^h for positive and negative hadrons. This difference is interpreted to indicate that a proton has a larger formation time than a pion.

Additional measurements of hadronization in various heavy nuclei with pion, kaon and proton identification are needed to clarify the issues raised by the present data concerning formation-time differences of different kinds of hadrons. Such measurements are underway at HERMES.

We gratefully acknowledge the DESY management for its support and the DESY staff and the staffs of the collaborating institutions. Additional support for this work was provided by the Deutscher Akademischer Austauschdienst (DAAD) and

INTAS, HCM, and TMR network contributions from the European Community.

References

1. A. Bialas, Proceedings of the Topical Conference on Electronuclear Physics with Internal Targets, January 1989, Stanford, California, Edited by R.G. Arnold, World Scientific, Singapore (1989), p. 65.
2. L.S. Osborne et al., Phys. Rev. Lett. **40** (1978) 1624.
3. EMC, J. Ashman et al., Z. Phys. **C 52** (1991) 1.
4. E665, M.R. Adams et al., Phys. Rev. **D 50** (1994) 1836.
5. B. Kopeliovich, J. Nemchik and E. Predazzi, Proceedings of the workshop on Future Physics at HERA, Edited by G. Ingelman, A. De Roeck and R. Klanner, DESY, 1995/1996, vol 2, 1038 (nucl-th/9607036); and B. Kopeliovich, J. Nemchik, private communication.
6. A. Bialas and T. Chmaj, Phys. Lett. **B 133** (1983) 241.
7. A. Bialas and M. Gyulassy, Nucl. Phys. **B 291** (1987) 793.
8. B.Z. Kopeliovich, Phys. Lett. **B 243** (1990) 141.
9. B.Z. Kopeliovich and F. Niedermayer, Sov. J. Nucl. Phys. **42** (1985) 504.
10. S.J. Brodsky and P. Hoyer, Phys. Lett. **B 298** (1993) 165.
11. S.J. Brodsky and A.H. Mueller, Phys. Lett. **B 206** (1988) 685.
12. L.L. Frankfurt et al., Ann. Rev. Nucl. Part. Sci. **45** (1994) 501; B.Z. Kopeliovich et al., Phys. Lett. **B 324** (1994) 469; P. Jain et al., Phys. Rep. **271** (1996) 67; O. Benhar et al., Journ. Exp. Theor. Phys. **84** (1997) 421.
13. T. Chmaj, Acta Phys. Pol. **B 18** (1987) 1131.
14. F.E. Low and K. Gottfried, Phys. Rev. **D 17** (1978) 2487.
15. N. Pavel, Nucl. Phys. **A 532** (1991) 465c.
16. E.L. Berger, Z. Phys. **C 4** (1980) 289.
17. HERMES, K. Ackerstaff et al., Nucl. Instrum. Methods **A 417** (1998) 230.
18. HERMES, K. Ackerstaff et al., Phys. Lett. **B 475** (2000) 386.
19. S. Barshay and D. Rein, Z. Phys. **C 46** (1990) 251; S. Barshay and G. Kreyerhoff, Phys. Lett. **B 487** (2000) 341.
20. G.A. Miller, S.J. Brodsky and M. Karliner, Phys. Lett. **B 481** (2000) 245.
21. A.A. Akhundov, D. Yu Bardin and N.M. Shumeiko, Sov. J. Nucl. Phys. **26** (1977) 660; D.Yu. Bardin and N.M. Shumeiko Sov. J. Nucl. Phys. **29** (1979) 499; and A.A. Akhundov et al. Sov. J. Nucl. Phys. **44** (1986) 988.
22. I. Akushevich, N. Shumeiko and A. Soroko, Eur. Phys. J. **C 10** (1999) 681.
23. B.Z. Kopeliovich, J. Raufeisen and A.V. Tarasov, Phys. Rev. **C 62** (2000) 035204.
24. B. Andersson et al., Phys. Rep. **97** (1983) 31.
25. J.J. van Hunen, Ph.D. Thesis, Utrecht University, March 2000.
26. B.Z. Kopeliovich, L.B. Litov, J. Nemchik, Int. J. Mod. Phys. **E 2** (1993) 767.
27. A. Bialas and J. Czyzewski, Phys. Lett. **B 222** (1989) 132; J. Czyzewski, Acta Phys. Polonica **B 21** (1990) 41; A. Bialas, Nucl. Phys. **A 532** (1991) 65c.
28. LEPTO: G. Ingelman, A. Edin and J. Rathsman, Comp. Phys. Comm. **101** (1997) 108.
29. Particle Data Group *Review of Particle Physics*, Phys. Rev. **D 54** (1996) 182.